GluR2 expressed by glial fibrillary acidic protein promoter decreases the number of neurons

Keisuke Tsuzuki[1], Shogo Ishiuchi[2]

[1]Department of Neurophysiology, Gunma University Graduate School of Medicine, Gunma 371-8511, Japan, [2]Department of Neurosurgery, Gunma University Graduate School of Medicine, Gunma 371-8511, Japan

TABLE OF CONTENTS

1. ABSTRACT

The alpha – amino–3 – hydroxyl – 5 –methyl - 4-isoxazolepropionic acid (AMPA) type ionotropic glutamate receptors participate in fast neuronal transmission. GluR2, a subunit of AMPA receptors, is the determinant of Ca^{2+}-permeability and surface expression of the receptors. To elucidate the role of AMPA receptors in the cells expressing glial fibrillary acidic protein (GFAP), we constructed mice expressing rat GluR2 cDNA under the control of a human GFAP promoter. The mice expressed approximately two folds increase of GluR2 in primary culture of astrocytes. Colocalization of GluR2 and GFAP was observed in Bergmann glial cells, which normally expressed AMPA receptors lacking GluR2. The diameter of glial fibers was significantly reduced and the leading edge of the processes was thinning or retracted in primary cultured BG cells. Interestingly, the transgenic mice had smaller brains compared with wild type mice. We found a 32% decrease in the number of cerebellar granule cells and a 31% decreases in cerebral cortical neurons. These results indicate that the increased expression of GluR2 in GFAP-positive cells alters neuron-glial interaction and leads to reduction in the number of neurons in adult mice.

2. INTRODUCTION

Glutamate is the major excitatory neurotransmitter in the central nervous system (CNS). AMPA receptors, the most abundantly expressed ionotropic glutamate receptors in the brain, mediate fast excitatory synaptic transmission in most neurons. AMPA receptors are composed of four subunits, GluR1, GluR2, GluR3 and GluR4 (1). The receptors assembled with the edited form of GluR2 exhibit little permeability to Ca^{2+}, whereas those lacking it are highly permeable to Ca^{2+} (2,3,4). In addition, GluR2 subunit plays important roles in surface expression of AMPA receptors. Constitutive delivery of AMPA receptors composed of GluR2/GluR3 assemblies to surface membrane regulates basic excitatory synaptic transmission. On the other hand, heteromeric GluR1/GluR2 assemblies form the reserve pools that are delivered activity dependently, which are essential in long term potentiation (LTP) in the hippocampus (5). In both constitutive and activity dependent conditions, GluR2 is required for surface expression of AMPA receptors and GluR2 deficient mice show reduced excitability in the hippocampus (6).
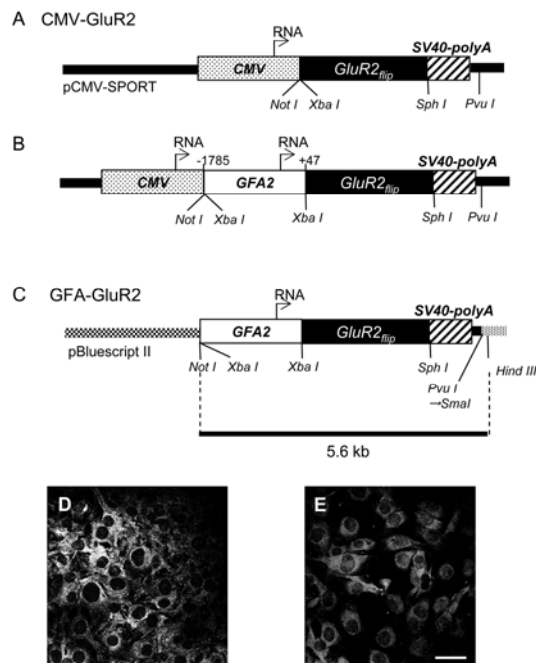
Figure 1. GFA-GluR2 construct. A. Diagram of the CMV-GluR2 construct. CMV-GluR2 construct contains a CMV promoter, GluR2 flip form cDNA, followed by a SV40 t-intron and polyadenylation signal. This plasmid was obtained by exchanging lac Z gene in pCMV-SPORT-beta GAL (Invitrogen) with GluR2 cDNA. B. Then, human GFAP promoter, GFA2, spanning bp -1785 to +47 relative to the transcriptional start site, the initiating ATG at +15 converted to TTG, was inserted into Xba-I site of the CMV-GluR2 construct. C. The GFA2-GluR2flip-SV40-polyA region was digested with Not I and Pvu I, Pvu I site was blunt ended, and subcloned into the Not I – Sma I site of a pBluescript II SK(-). Finally, a 5.6 kb construct between Not I and Hind III was purified and injected into fertilized oocytes of C57BL/6 mated with DBA/2. D. Expression of GluR2 in a CMV-GluR2 transfected gliobastoma cell line, CGNH-89, which expresses GFAP but lack the expression of GluR2. E. Expression of GluR2 in GFA-GluR2 transfected cells. No immunoreactivity was seen in untransfected cells (data not shown). Scale bar, 50 micrometer.

Although AMPA receptors participates in synaptic transmission between neurons, the expression of AMPA receptors are not restricted in neural cells. Bergmann glial cells (BG) in the cerebellum express AMPA receptors composed of GluR1 and GluR4 (7,8). The GluR2-lacking AMPA receptors are expressed all along BG processes, which engulfs small excitatory synapses (9). Reduced Ca^{2+} permeability of these receptors leads to changes in BG morphology and decreases coverage of excitatory synapses (10), indicating the presence of the glial coverage through AMPA receptors is essential for excitatory synaptic transmission.

GluR2 is the most important subunit in neuronal functions, however, the roles of AMPA receptors in glial cells have been not fully examined. We previously reported that the alternation of GluR2 expression by a viral vector in glial cells *in vivo* and *in vitro* caused marked morphological changes of glial fibers (8,10). In this study, we examined the role of glial cells by modulating the expression of GluR2 under the promoter of human GFAP (11). The mice expressed GluR2 in BG cells and in type-1 astrocytes, under the control of GFAP promoter. Although the mice developed normally without showing gross abnormalities, neuro-glial interaction was altered. We found decreases of neurons in the cerebellar granule cells and in the cerebral cortex.

3. MATERIALS AND METHODS

3.1. Gene constructs

CMV-GluR2 gene construct and GFA-GluR2 gene construct: A plasmid containing rat GluR2, which was edited at Q/R RNA editing site (12,13), edited at R/G RNA editing site (14) and in the flip splicing variant (13) was kindly gifted from Drs. Michael Hollmann (Ruhr University Bochum, Germany), Jim Boulter and Stephan Heinemann (Salk Institute, CA) (15). The 2.8 kb Not I – Sph I GluR2 cDNA was subcloned into NotI - Sph I in a mammalian expression vector pCMV- SPORT - beta GAL (Invitrogen, Carlsbad, CA), obtaining pCMV - SPORT - GluR2. This expression vector, CMV-GluR2 gene construct, possesses cytomegalovirus promoter, SV40 intron and polyadenylation signal (see Figure 1). GFA-GluR2 gene construct was obtained by exchanging cytomegalovirus promoter with GFAP promoter. A plasmid containing the promoter of human GFAP promoter was kindly gifted from Dr. Michael Brenner (University of Alabama at Birmingham, AL) (GFA2-lacZ, (11). The region containing human GFAP promoter (-1785 - +47) was digested with Xba I and subcloned into Xba I site which exists between CMV promoter and GluR2 of pCMV-SPORT-GluR2 (Figure 1B). CMV promoter was removed as follows. The GFAP promoter - GluR2 cDNA - SV40 intron and polyadenylation signal was cut with Pvu I, blunt ended with T4 DNA polymerase (Takara, Ohtsu, Japan), digested with Not I and subcloned between Not I - Sma I of a pBluescript SKII- vector (Stratagene, La Jolla, CA), obtaining GFA-GluR2 (Figure 1C).

3.2. Transfection of gene constructs to GFAP expressing cells

CGNH-89 cells are a human glioblastoma cell line established by Ishiuchi *et al*. The day before transfection, 10^5 cells were plated on a 35 mm culture dish (Falcon - Beckton-Dickinson, San Jose, CA). On the day of transfection, 3 microlitter of a transfection reagent (FuGene 6, Roche Diagnostics, Indianapolis, IN) was mixed to 100 microlitter Dulbecco Modified Eagle Medium (Low glucose, Invitrogen) and 1 microgram of either CMV-GluR2 or GFA-GluR2 gene construct was added. After incubation at room temperature for 30 minutes, the mixture was added to the culture dish drop-wisely and incubated for 48 to 60 hours. The cells were fixed with 4% paraform-aldehyde containing PBS, and the expression of GluR2 was determined by fluorescent immunohistochemistry.

3.3. Construction of transgenic mice

GFA-GluR2 was digested with Not I and Hind III, obtaining 5.6 kb construct (see Figure 1). After GEL purification using QIA quick GEL Extraction Kit (Qiagen, Hilden, Germany), the construct was diluted with PBS at concentration of 4 ng / mL and injected into the male pronuclei of fertilized oocytes, obtained from C57BL/6Cr Slc mated with DBA/2 Cr Slc (Japan SLC, Hamamatsu, Japan). After incubation in mWM medium (in mM, NaCl 110, KCl 4.8, KH2PO4 1.2, Ca-lactate 1.5, MgSO4 1.2, NaHCO3 22, glucose 5.5, Na-pyruvate 0.22, EDTA-2Na 0.05, 2-mercaptoethanol 0.05, supplemented with 0.3% BSA, penicillin-G 8 mg / 100 mL-streptomycin 5 mg / 100 mL) overlaid with mineral oil at 37ºC in 5% CO2 incubator, the two-stage eggs were transferred into oval ducts of pseudopregnant ICR mice. Founder transgenic mice were identified by PCR analysis of genomic DNA from tail biopsies prepared by enzymatic extraction (Extract-N-Amp Tissue PCR Kit, Sigma, Saint Louis, MO). A primer pair that amplifies rat GluR2 cDNA (2R2up 5'-TTG TTG GAG GTG TGT GGT GGT TCT TTA C-3' and 2R2lo 5'-CAT TGT GGA CTC CAG CAA GTC CCA TAC-3') was used. PCR amplification was performed in PCR buffer containing 50 mM KCl, 1.5 mM MgCl2, 20 mM Tris-HCl (pH8.3), 0.1 micromolar primers, 50 micromolar dNTPs, and 0.25 U Taq DNA polymerase (Sigma) in a 10 microlitter reaction volume under the following reaction conditions: initial denaturation at 94ºC for 2 min, 30 cycles of denaturation at 94ºC for 15 sec, annealing at 55ºC for 15 sec, and extension at 72ºC for 20 sec, followed by a final extension at 72ºC for 4 min. Amplification products with an expected length of 325 bp were analyzed by electrophoresis on 1.5% agarose gels containing 0.5 microgram / mL etidium bromide in tris-borate buffer (0.5 x TBE).

3.4. Animals

Transgenic (TG) mice and wild-type (WT) C57BL/6 Cr SLC mice were bred at Gunma University Institute for Animal Research. Holding rooms were maintained at a constant temperature (25 ± 5°C) and humidity (50 ± 10%), and lights were on for 12 hr (starting at 6:00 A.M.). Mice were allowed access to standard lab chow and water *ad libitum*. TG mice mated with C57BL/6 for nine generations or more were used for the experiments. All experiments were approved by the Gunma University Ethics Committee of Aminal Experiments and the Gunma University Biosafety Commetee for Genome Research and were performed under the laws of Japan.

3.5. Culture of cerebellar Bergmann glia and forebrain astrocyte

Culture of BG cells was performed as reported previously (8). Briefly, newborn mice (P1) or mice on postnatal day 2 (P2) were anesthetized with dimethylether. After removing the brain, the cerebellum was quickly dissected into approximately 1-mm cube by sterile scalpel blades and plated on a 25-cm² culture flask (Falcon), with the medium just cover the cube. The tail was used for genotyping.

Forebrain astrocytes were obtained from P1 or P2 mice as reported previously (16). Briefly, the forebrain was quickly cut into small pieces and incubated with 1 mL of 0.25% collagenase in Hanks Balanced Salt Solution (HBSS, Invitrogen) for 30 minutes at 37ºC. The cells were collected with centrifuge of 120 g for 5 minutes. The cell pellets were suspended in 2 mL of 0.25% trypsine - 1 mM EDTA and incubated for 3 minutes. Then, 2 mL of DMEM containing 10 % fetal bovine serum (FBS) was added and pipetted 5 ~ 10 times The cells were collected with centrifuge of 120 g for 5 minutes and re-suspended to 2 mL of DMEM containing 10 % FBS and plated to a 25-cm² flask. When culture was confluent at ~10 days, the lid of the flask was sealed firmly, wrap with parafilm and taped to a rotary platform and rotated at 150 rpm for 16 hours at 37ºC. After removing supernatant and replacing it with DMEM containing 10 % FBS with 20 micromolar cytosine arabinoside (Ara C, Sigma), the cells were cultured for 48 hours at 37ºC in CO2 incubator. Then, medium was changed to fresh DMEM containing 10 % FBS and cultured for 24 hours. After treatment of Ara C again and the cells were trypsinized and plated on a 75-cm² flask containing 10 ml fresh DMEM supplemented with 10 % FBS. The culture was confluent at ~4 days. This procedure yielded cultures of nearly pure type-1 astrocytes.

3.6. Quantitative RT-PCR

RNA extraction was performed as reported previously (17). After removing the medium of a type-1 astrocyte culture in a 75-cm² flask, RNA was extracted with 1 mL of Trizol Reagent (Invitrogen) according to the vender's instruction. Brain RNA was extracted as follows. The cerebellum of TG and WT mice were homogenized in 400 microlitter of Trizol Reagent with a Dounce homogenizer. Undispersed mass was removed by a brief centrifuge (5000 g, 1 min) and RNA extraction was proceeded. After treatment with DNase I (Invitrogen, amplification grade), the amount of RNA was quantified with UV spectrometer and the quality was determined with agarose gel electrophoresis. Reverse transcription (RT) was performed as follows. RNA (1 ~ 2 microgram), random hexamor (pdN6, 0.2 nmol, Roche Diagnostics), dATP, dCTP, dGTP and dTTP (10 nmol each, GE Healthcare, Amersham, UK) were mixed in a 10 microlitter-reaction volume and incubated at 70ºC for 5 minutes and quickly chilled on ice. Then, M-MLV (Invitrogen, 200 units), DTT (final 10 mM) and buffer supplied by the distributor were added and incubated for 22ºC 5 minutes followed by 37ºC 30 minutes.

Three methods were used for the quantification of GluR2 mRNA in the present study, limiting dilution analysis and real time quantitative PCR. Limiting dilution analysis was performed as follows. The reverse transcribed products were serially diluted in (in input RNA) 10, 3.16, 1, 0.316 and 0.1 pg. The following primer sets were used. GFAP-up 5'- CCG CTT CCT GGA ACA GCA AAA C; GFAP-lo CCT CCA GCG ATT CAA CCT TTC TCT for GFAP detection. 2R3-up 5'- TGG AGG TGT GTG GTG GTT CTT TAC; 2R3-lo 5'-GTG GAC TCC AGC AAG TAG GCA TAC for GluR2 detection. Serial dilution of the template caused drop-outs of amplified products according to Poisson's distribution (18). The rates of drop-outs were

measured and the median detective amounts were estimated using the Spearman-Karber formula (19).

Real time quantitative PCR (20) was performed using ABI PRISM 7500 system (Applied Biosystems, Foster City, CA). Briefly, RT products of type I astrocyte culture were serially diluted to 80, 40 20, 10, 5 and 2 ng, and compared with 20 ng of type I astrocyte culture of transgenic mice and dissolved in Universal Mastermix (Applied Biosystems) in the final reaction volume of 20 microlitter. A TaqMan probe for mouse GluR2 (Mm00442822_ml, Applied Biosystems, FAM labeled, MGB quencher) was used to quantify GluR2 cDNA and VIC-MGB 18S rRNA probe was used to normalize the amounts of imput RNA. The thermal cycling condtions included 2 min at 50ºC and 10 min at 50ºC. Thermal cycling proceeded with 40 cycles of 95ºC for 15 sec and 60ºC for 1 min, and fluorescence for FAM and VIC were detected at the 60ºC stage. Amounts of GluR2 normalized by 18S rRNA were calculated according to the vender's instruction (User bulletin #2, ABI PRISM 7700 Sequence Detection System).

Competitive PCR analysis among GluR1-R4 was performed as reported previously (2,21,22). RT products of the cerebellum were amplified with a primer pair that amplifies cDNAs of all subunits of AMPA receptors, GluR1, GluR2, GluR3 and GluR4, at the same efficiency (17). To determine the relative amounts of each subunit the amplified fragments were digested with subunit specific restriction enzymes, Bgl I, Bsp 1286 I, Eco 47III and Eco RI, which selectively digest cDNAs of GluR1, GluR2, GluR3 and GluR4, respectively. The intensity of bands was quantified by a Quantity-One software (BioRad, Hercules, CA).

3.7. Immunoblotting

The forebrain and the cerebellum of TG and WT mice were homogenized in 400 microlitter of ice-cold TBS (150 mM NaCl, 20 mM Tris HCl, pH 7.5) with polytron homogenizer. Then 400 microlitter of 2x Sample buffer (Wako, Osaka, Japan, 125 mM Tris-HCl, 4% SDS, 20% Glycerol, 0.002% BPB, 10 % 2-mercaptoethanol, pH6.8). Type I astocytes in a 75-cm^2 flask were detached with cell scraper and collected by centrifuge, suspended in 400 microlitter of ice-cold TBS, then 300 microlitter of 2x Sample buffer was added. The content of protein was quantified with the Bradford method (Dojin, Kumamoto, Japan). The lysate was then denatured at 95ºC for 2 min and loaded onto 5 - 20% polyacrylamide gradient gels. Twenty micrograms of proteins were fractionated by sodium dodecyl sulphate polyacylamide gel electrophoresis (SDS-PAGE), and transferred to PVDF membrane (Millipore, MA) by using the TE-70 Series SemiPhor Semi-Dry Transfer Unit (GE Healthcare). The membranes were incubated with goat GluR2 antibody (GluR-2 (N-19), Santa Cruz Biotechnology, Santa Cruz, CA), rabbit actin antibody (Sigma) and rabbit GluR4 antibody (Chemicon, Temecula, CA) in a blocking buffer consisting of TBS containing 0.1% I-block (Applied Biosystems), 0.02% Tween-20 for 1 hour. After incubation with species-specific HRP-conjugated secondary antibodies (Dako, Glostrup, Denmark) for 15 min, the ECL Western blotting detection system (GE Health care) was applied. The chemiluminescence was detected using a CCD camera (ChemiDoc XRS, BioRad). The intensity of bands was quantified by a Quantity-One software (BioRad).

3.8. Immunohistochemistry

Cultured cells were fixed by ice-cold PBS containing 4% paraformaldehyde (4% PFA) for 15 min, permealized by 0.1% Triton X-100 in PBS for 15 min, and succeeded for immunohistochemistry. To obtain brain sections, animals were deeply anesthetized with pentobarbital. Then 25 ml of 100 mM phosphate buffer (pH7.4), followed by 40 ml of ice-cold 4% PFA was perfused transcardially. The brain was removed and immersed in ice-cold 4% PFA for 1 hour. Then, saggital sections, 100~400 micrometer thickness, were prepared with a vibratome slicer (Vibratome 3000, Vibratome Co., St Louis, MO). Then the slices were permeabilized by 0.1% Triton X-100 in PBS for 30 min.

Nonspecific stainings were blocked by 10% Donkey serum for 1 hour. The following antibodies were used; rabbit GFAP antibody (1:100; DAKO), goat GluR2 antibody (1:100, Santa Cruz), rabbit GluR2 antibody (1:100, Chemicon), rabbit calbindin antibody (1:100, Sigma). Primary antibodies were applied for overnight at 4 – 8 ºC. Reactions were detected by incubation for 1-h with donkey anti-rabbit IgG conjugated to Alexa 488 or Alexa 594 (1:500, Invitrogen) or donkey anti-rabbit IgG conjugated to Alexa 488 or Alexa 594 (1:500, Invitrogen). For non-reactive control, primary antibodies were omitted. The fluorescent signals were viewed with a laser-scanning confocal microscope (Pascal, Zeiss, Jena, Germany).

3.9. Histology

Histological preparation of the cerebellum and the cerebral cortex were obtained as reported previously (23). Brains fixed in 4% PFA (see above) were embedded in paraffin. Sections were cut at 3 micrometer and stained with hematoxylin-eosin (H & E),

3.10. Statistics

Statistical analysis was performed with software (StatView 5.0-J, SAS Institute Inc, Cary, NC, USA). All data were shown in mean ± SEM. Relative changes in TG mice normalized with WT mice were determined by dividing the average TG value by the average WT value. The standard deviation of the quotient was calculated from the standard deviations (SD) of the TG and WT values using the following formula.

$$SD = \overline{X} \cdot cv = \overline{X} \cdot \sqrt{cv_1^2 + cv_2^2}$$

where $\overline{X}$ was the mean of TG divided by the mean of WT, $cv1$ and $cv2$ are the standard deviation of TG and WT. SEM was obtained by dividing SD by the square root of $(n_1 + n_2)/2$, where n_1 is the trials of TG and n_2 is that of WT, respectively.

4. RESULTS

4.1. GFAP promoter induced GluR2 expression in glioblastoma cells

A human GFAP promoter (11) was used for cell specific expression of GluR2 in the present study. Although this promoter has been used in many reports to express foreign genes such as Lac Z (11), green fluorescent protein (GFP) (24,25), Cre (26), herpes simplex virus thymidine kinase (27) in cells of glial-lineage, expressions of intrinsic genes have not been examined. Since GluR2, an intrinsic gene abundantly expressed in the brain, was subjected to be expressed in a cell specific manner, we examined whether the promoter is powerful enough to be detected in immunoblotting and in immunohistochemisty. For this purpose, we constructed GluR2 expression construct firstly under the control of the CMV promoter, a powerful viral promoter, then the promoter was replaced with that of GFAP (Figure 1A-C).

CGNH-89 is a human glioblastoma cell line that expresses GFAP and AMPA receptor subunits GluR1 and GluR4, lacking the expression of GluR2 (28). Either CMV-GluR2 or GFA-GluR2 gene construct was transfected and expression of GluR2 was examined with immunohistochemisty (Figure 1D, E). GluR2 expression was detected in both CMV-GluR2 and GFA-GluR2 transfected cells. Although the intensity of GluR2 immunofluorescence was approximately three folds stronger in CMV-GluR2 transfected cell, matching with the report showing lower power of the GFAP promoter compared with that of CMV promoter (29), the expression of GluR2 in soma was clearly detected in GFA-GluR2 transfected cells.

The GFA-GluR2 construct was linealized by digestion, purified and used for creation transgenic mice (Figure 1C).

4.2. Establishment of GFA-GluR2 Transgenic mice

Transgenic mice were generated by microinjection of fertilized mouse oocytes. We transferred 277 blastocytes in 10 psudopregnant mice, obtaining 43 offsprings. Founder transgenic mice were identified by PCR analysis of genomic DNA from tail biopsies. We obtained seven lines of founders that the GFA-GluR2 were transferred. These founder mice were mated with C57BL/6 and offsprings were subjected to examine the expression of GluR2 in the brain. Three of the seven transgenic lines expressed GluR2 in BG cells. Distributions of GluR2 positive BG cells in these three lines were similar. Intensities of GluR2 expressions, examined with fluorescence intensities of the secondary antibodies, also did not differ among three lines. One line was selected and mated with C57BL/6 mice for more than nine generations, which were subjected for experiments. These TG mice grew up normal and were fertile. No differences were seen in body size compared to WT C57BL/6 mice. The body weights of six-weeks old TG mice were (in gram) 20.8 ± 0.4 (n = 9) and 18.3 ± 0.7 (n = 12), male and female, respectively, and that of WT mice were 20.7 ± 0.3 (n = 13) and 18.1 ± 0.5 (n = 12), respectively.

4.3. Increased GluR2 expression in cultured type I astrocytes

Expression of GluR2 in GFAP- positive cells were examined in type-1 astrocytes and cultured BG cells. First, quantitative examination of GluR2 was performed in cultured type-1 astrocytes. Type-1 astrocytes comprise the large majority of glial cell in the brain and nearly pure population of type-1 astrocytes could be obtained in adherent culture (16). We examined increases of GluR2 mRNA and protein in cultured type-1 astrocytes of TG mice. Amounts of GluR2 mRNA in cultured type-1 astrocytes was determined with two different ways, real time quantitative PCR (20) and limiting dilution analysis of cDNAs. RNA was prepared from three independent cultures (see methods). In real time quantitative PCR, serially diluted cDNAs of WT culture, 80, 40, 20, 10 and 5 ng and 20 ng cDNAs of TG culture were subjected to simultaneous amplification of cDNAs of GluR2 and 18S ribosomal RNA using TaqMan probes. We found 1.88 ± 0.16 (n = 3) folds increases of GluR2 cDNA in TG culture normalized with 18S ribosomal RNA (Figure 2A).

For limiting dilution analysis, cDNAs of both WT and TG culture were diluted and subjected to PCR that amplifies cDNAs at the single molecule level. Serial dilution of the template caused drop-outs of amplified products according to Poisson's distribution, indicating the absence of targets in the reaction tube (18). The rates of drop-outs were measured and the median detective amounts were estimated using the Spearman-Karber formula (19). The median detective amounts of GluR2 in WT culture was 2.31 pg total RNA (n=8), where as that in TG culture was 1.15 pg (n=8), indicating 2.1 folds increases of GluR2 mRNA in TG culture (Figure 2A).

The increases of GluR2 mRNA in TG culture resulted in the increases of GluR2 protein. Figure 2B shows the results of immunoblotting. Here, the results of two independent cultures of each were shown. Although the amount of GluR2 expressed in cultured astrocytes were not abundant, 108-kD bands of GluR2 were seen. The blots of GluR2 were obviously increased in TG culture (Figure 2B). Increases of GluR2 blotting in TG culture normalized with actin blotting was 4.2 ± 1.0 folds (n=8). These results clearly showed that GFA-GluR2 construct induced GluR2 expression in GFAP expressing cells.

4.4. Increased GluR2 expression influenced BG-granule cells interaction

Primary cultured BG cells were obtained from explant cultures from newborn mice (8). As shown in Figure 3, elongating glial fibers of BG cells expressed GFAP (Figure 3B), and GluR2 was not expressed in glial fibers in WT mice but expressed in granule cells (Figure 3A). In contrast, BG cells of TG mice expressed both GluR2 (Figure 3G) and GFAP (Figure 3H). Next, we examined the number of granule cells migrating onto the guiding substrate of BG fibers radial away from an explant during the 5 days from plating using time-lapse microscopy (Figure 3C-F, 3I-N). The diameter of glial fibers was 125 ± 24
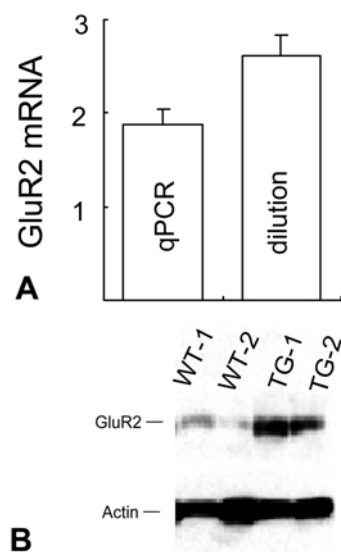
Figure 2. Increased GluR2 in type-1 astrocytes of TG mice. A. GluR2 mRNA in cultured type I astrocyte. Relative amounts of GluR2 obtained from TG cultures against that from WT cultures were shown. qPCR shows the folds increases determined with real time quantitative PCR. Dilution shows the folds increases of GluR2 determined by the median detective amounts estimated by the Spearman-Karber formula. B. Immunoblotting. Cell lysates of cultured astrocytes were separated on SDS-PAGE and immunoblotted with GluR2 antibody and actin antibody. Blottings of two independent cultures of both WT and TG were shown.

micrometer in WT mice (n = 6) and 38 ± 11 micrometer in TG mice (n = 6). BG cell from TG mice significantly reduced the diameter of the processes compared with that of WT mice (p < 0.05, Student's t-test). Moreover, leading edge of the processes in WT mice was healthy and represented growth-cone like extension with branching, but in TG mice, the tip was thinning or retracted. We also found reduced number of granule cells attached to glial fibers of BG cells in TG mice. Here, 23 ± 8 (n = 6) granule cells were attached to 20 x 20 micrometer region of glial fiber in WT, whereas only 8 ± 2 (n = 6) granule cells were attached in TG. Motility of granule cells was influenced by the alternation of BG fibers. Granule cells moved bidirectionally onto the substrate, and they settled down onto the bottom of flask along the branched fibers. In TG mice, migratory granule cells could not settle down onto the destination, because the substrate fibers were retracted, and they remained in the abnormal tip of the processes (Figure 3N). Therefore, GluR2 expression in BG fibers changed migratory behaviour of granule cells, being influenced by the morphological alternation of BG fibers.

4.5. GluR2 expression in TG mice

GluR2 is abundantly expressed in almost all neurons in the brain and most of GluR2 expressed in the brain is derived from neurons. Brains of adult (postnatal age 6 - 9 weeks) were subjected to RT-PCR and immunoblot analyses. Competitive RT-PCR analysis using a primer set that amplifies all AMPA receptor subunit simultaneously at the same efficiency allows one to determine relative abundance of GluR1 – GluR4 mRNA (17,21,22). The relative abundance of GluR1 – GluR4 mRNA in the cerebellum of WT and TG mice were determined in Figure 4A and 4B. The most abundant mRNA in WT cerebellum was GluR1, followed by GluR4 and GluR2 (Figure 4A). The order was not changed in TG cerebellum. The relative abundance of GluR1 – R4 in WT cerebellum was 43 ± 5%, 18 ± 2%, 5 ± 2%, 34 ± 7% (n=4), GluR1, GluR2, GluR3 and GluR4, respectively, and that in TG cerebellum was 42 ± 8%, 21 ± 5%, 4 ± 2%, 33 ± 8% (n=4). Significant increases of GluR2 were not detected in mRNA of the cerebellum in TG mice.

Figure 4C shows the results of immunoblotting. Here, the results of forebrain and cerebellum in two animals of each were shown. The amount of GluR2 protein in TG was similar with that in WT mice in both forebrain and cerebellum. The relative amounts of GluR2 protein of TG mice normalized with actin were 97 ± 17% (n=5) and 106 ± 24% (n=5) of that of WT mice in the cerebellum and in the forebrain, respectively.

Some subunits of AMPA receptors are reported to express differently among brain region. As shown in Figure 4C, GluR2 was abundantly expressed both in the forebrain. The amounts of GluR2 in the forebrain relative to cerebellum were 121 ± 12% (n=5) and 106 ± 6% (n=5) in both WT and TG, respectively. GluR4 was abundantly expressed in the cerebellum. The amounts of GluR4 in the forebrain relative to cerebellum were 14 ± 3% (n=5) and 9 ± 2% (n=5) in both WT and TG, respectively, indicating that proportion of AMPA receptor subunits were not changed in the TG mice.

These results indicates that expression of GluR2 occurred in GFAP expressing cells did not alter the total expression of GluR2 in brain, indicating that the increased expression of GluR2 was not occurred in neuronal cells that supply most of GluR2 in the brain and the increased expression was restricted in the glial cells.

4.6. GluR2 immunostaining in the cerebellar cortex

BG cells in the cerebellum abundantly express AMPA receptors composed of GluR1 and GluR4, lacking the expression of GluR2 (3). Expression of GluR2 in BG cells of TG mice was examined with immunohistochemistry. Figure 5A shows the expression of GluR2 in WT mice. GluR2 was strongly expressed in the cell bodies and dendrites of Purkinje cells. Granule cells also expressed GluR2. Radial fibers of BG cells did not expressed GluR2, which was shown as black vertical stripes in Figure 5A. In TG mice amount of GluR2 expressions in the molecular layer was increased. Radial fibers of BG cells expressed GluR2 (Figure 5B), and vertical stripes were lost.

Unexpectedly, expression of GFAP was changed in TG mice. Focal increases of GFAP were seen near the surface of cerebellar cortex in addition with the regular vertical expression in radial fibers of BG cells and the
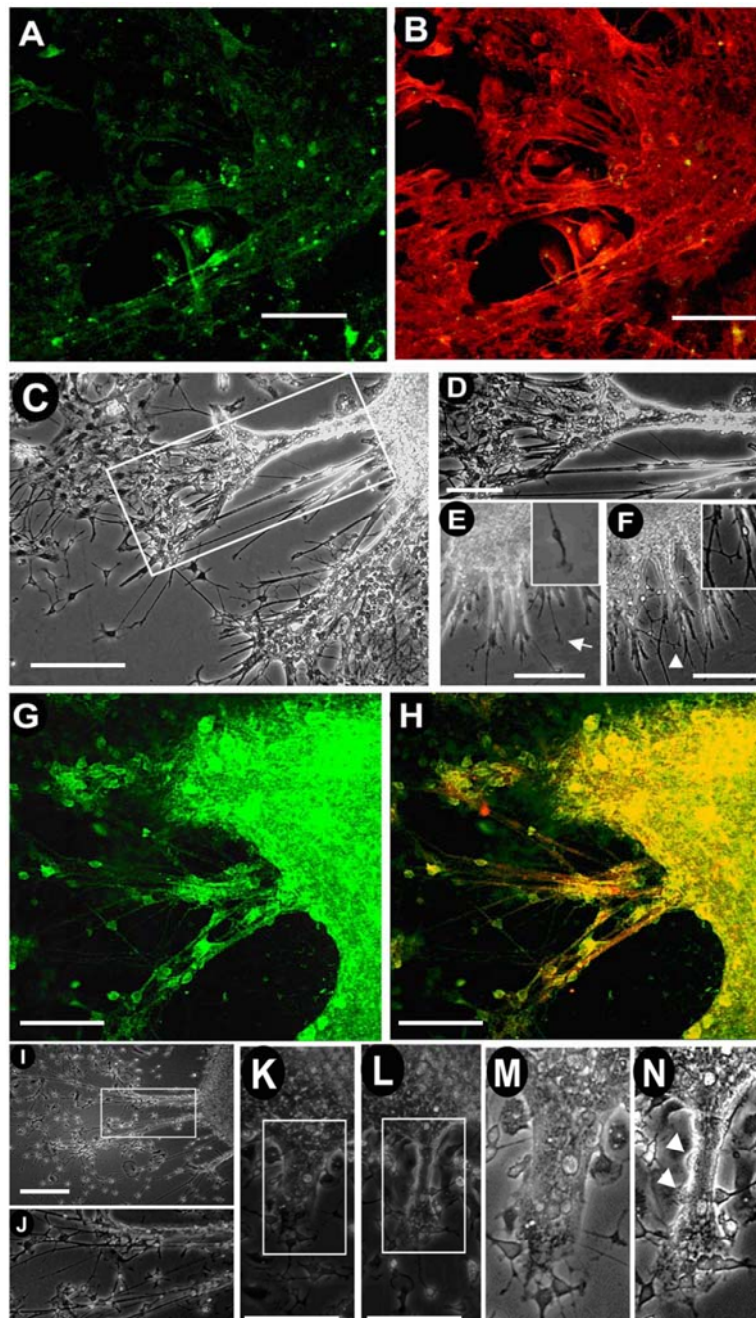
Figure 3. Expression of GluR2 in cerebellar explant culture. A. Expression of GluR2 and GFAP in cerebellar explant culture form wild type (WT) mice. Cultured BG cells were obtained from explant cultures from the cerebellum of newborn mice. GluR2 was expressed only in cerebellar granule cells attached to glial fibers (A, green), since Bergmann glial (BG) cells lack the expression of GluR2. B. Expression of GFAP (red) merged with GluR2 expression (Green). C. Phase-contrast image of glial fibers of BG cells emerged from an explant. D. Enlargement of the box shown in C. Cell with bright soma were migrating granule cells onto Bergman glial fibers. E-F Glial processes of WT mice in a 12 hours interval using time-lapse microscope. Note the extension (arrow in E) and branching (arrowhead in F) of growth-cone like leading edges. See insets of E and F for their magnification. G-H, Expression of GluR2 (G) and a merged image with GFAP in TG mice (H). BG cells of TG mice expressed both GluR2 (green) and GFAP (red). I. Phase-contrast image of glial fibers in TG mice. The diameter of the bundles in glial fibers was reduced in BG cells of TG mice. J. Enlargement of the box shown in I. The tip of leading edge was thinning or retracted. K-L. Leading edge of the processes in TG mice in a 12 hours interval using time-lapse microscope. M, N. Enlargement of the box shown in K, L, respectively. Note migratory granule cells could not settle down onto the destination (arrowheads). Scale bars indicate 100 micrometer.
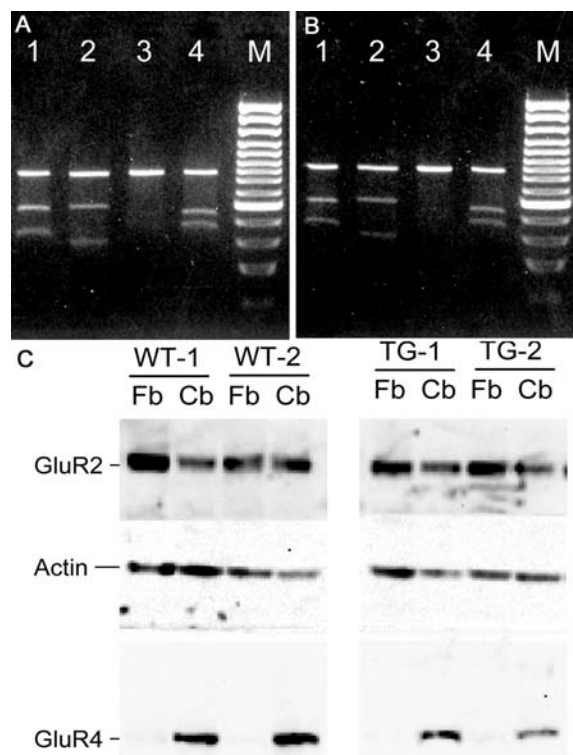
Figure 4. Expression of GluR2 mRNA and protein in WT and TG mice brain. A-B. Relative abundance of GluR2 over GluR1-GluR4 was determined by RT-PCR followed by restriction analysis. Cerebellar RNA from WT (A) and TG (B) 8-weeks-old mice were prepared and RT-PCR were performed with a primer set that amplifies GluR1-GluR4 at the same efficiencies. The obtained fragments (750 bp) were digested with subunit specific restriction enzymes. Lane 1, digestion with GluR1 specific enzyme Bgl I. Lane 2, digestion with GluR2 specific enzyme Bsp1286 I. Lane 3, digestion with GluR3 specific enzyme Eco47 III. Lane 4, digestion with GluR4 specific enzyme EcoR I. Note the most abundantly expressed subunit in WT cerebellum was GluR1, followed by GluR4, then GluR2. The order was not changed in TG. M indicates molecular weight marker, 100 bp ladder. C. Immunoblotting. Cell lysates of forebrain and cerebellum of WT (left) and TG (right) mice were separated with SDS-PAGE and immunoblotted with GluR2 antibody, actin antibody and GluR4 antibody. Two samples were prepared for both WT and TG.

regular expressions in ependymal cells (30) (Figure 5C). The focal expressions of GFAP were found in all three lines obtained in the present study. Expression of GluR2 was increased in these focuses of GFAP (Figure 5D,E), performing GluR2 focus.

Calbindin is selectively expressed in Purkinje cells in the molecular layer. The fine dendrites of Purkinje cells were not affected by the focal increment of GluR2 (Figure 5F-H).

4.7. Smaller brain in TG mice
Although gross abnormalities in the brain were not seen and no differences were seen in the size of body,

we found small but clear changes in the size of brain. Figure 6A shows a top side view of WT (left hemisphere) and TG (right hemisphere). The cerebral cortex and the cerebellum of TG mice were smaller than that of WT. Figure 6B shows the down side view of WT and TG. An anterior-posterior axis of the forebrain was shortened in TG mice. The size of cerebral cortex was reduced. On the other hand, the brainstem of TG mice seems not to be affected, inducing disproportion of the brain.

The weight of TG cerebellum (in mg. 56.3 ± 5.3, n=7) was significantly lighter than that of WT (72.9 ± 3.2, n = 7) (Figure 6C). The weight of forebrain also has the tendency of lighter, $92.7 \pm 3.3\%$ (n = 7) of WT. In spite of the changes in the cerebellum and in the forebrain, differences of weight of the brainstem in TG mice was not observed, $98.7 \pm 2.7\%$ (n = 7) of WT.

4.8. Decreased neuron number in cerebellum and in cerebral cortex
Changes in the brain were further examined in thin sections. The smaller sized of brains did not reveal gross abnormalities. In the cerebellum, widths of the molecular layer and granule layer in TG were thinner to ~90% of WT (Figure 7A and B). The proportion of the widths of layers was not changed. Higher magnification views are shown in Figure 7C and D. Although there are almost no differences in the number of cells in the molecular layer, the number of granule cells in TG was significantly reduced. The number of cells in a restricted area, 50 micrometer x 50 micrometer x 3 micrometer, of the cerebellum in the granule cell layer in WT was 73.0 ± 3.2 (n=4), whereas 49.7 ± 2.7 (n=4) in TG (Figure 7E). The number of cells in the molecular cell layer was not significantly different, 22.3 ± 0.3 (n=4) and 20.3 ± 1.5 (n=4), in WT and TG, respectively.

Cerebral cortex of TG mice was also affected. Figure 8A shows the somatosensory cortex of WT and TG. The numbers of neurons are decreased in all layers of the cerebral cortex. The numbers of cells in 150 micrometer vertical lengths, including cells in layer I to V, and 50 micrometer widths in WT was 153.2 ± 7.4 (n=4) and 105.8 ± 7.0 (n=4), in WT and TG, respectively.

5. DISCUSSION

We constructed TG mice that expressed the flip form of rat GluR2 under the control of a human GFAP promoter. The mice expressed GluR2 in both intrinsically GluR2 expressing astrocytes and GluR2 lacking BG cells. The mice irregularly expressed GFAP in the cerebral cortex (Figure 5) and the cell numbers in cerebellum and cerebral cortex were reduced (Figs 7-8).

5.1. Powers of GFA2 promoter
Although the human GFAP promoter, GFA2, induced expression of GluR2 in a glioblastoma cell line that lack the expression GluR2 (Figure 1E), the expression of GluR2 was lower than that of CMV promoter, a viral promoter frequently used in transfection in mammalian cells (Figure 1D). de Leeuw *et al* have reported that the
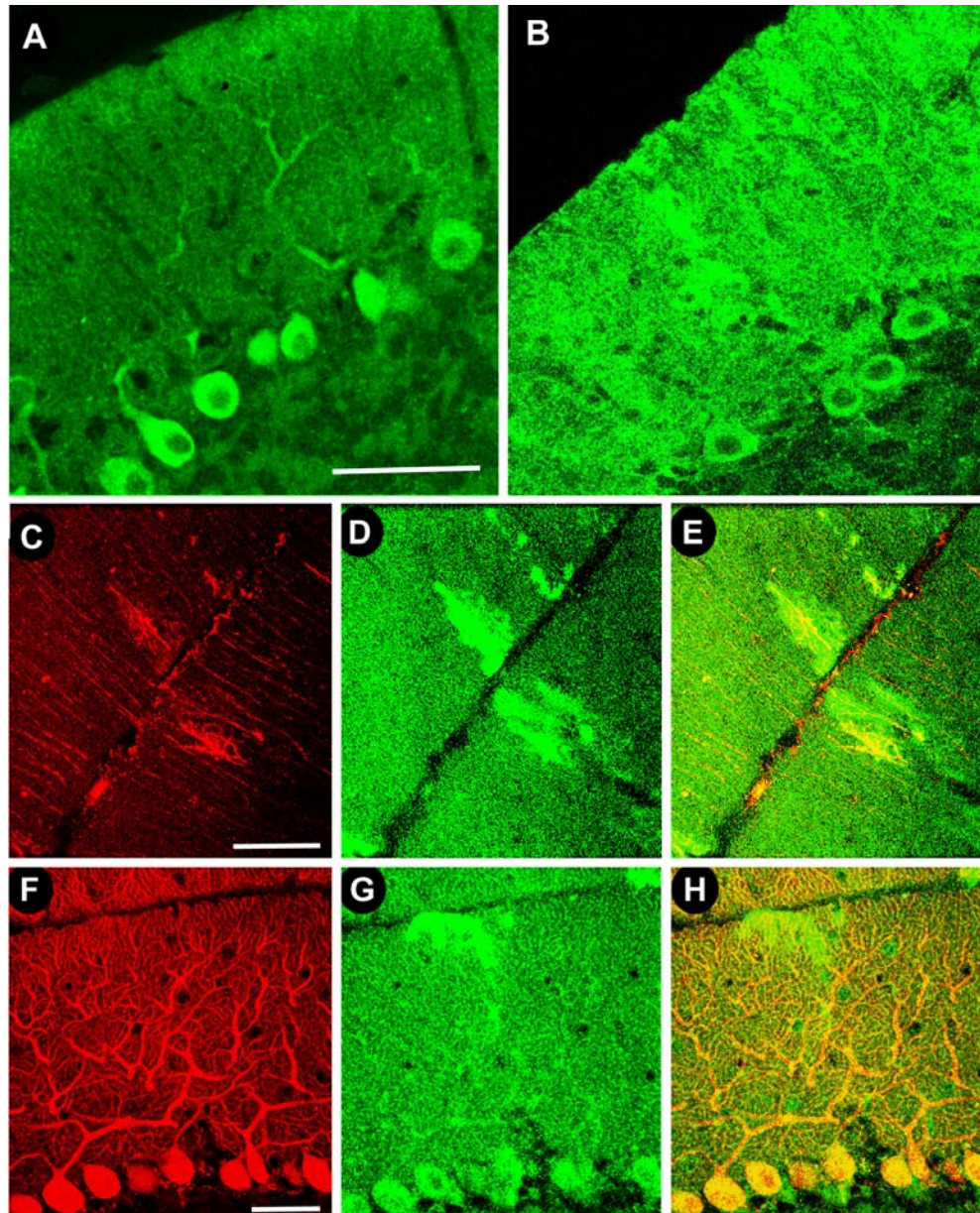
Figure 5. Increases of GluR2 expression in the cerebellar cortex in TG mice. A-B. Cerebellar cortex of WT (A) and TG (B) was stained with GluR2 antibody. The fluorescence intensities were normalized at the soma of Purkinje cells in both panels. Note higher GluR2 expression in the molecular layer in TG. C. GFAP expression in TG mice. In addition with thin vartical expressions, focal wedged shaped expressions of GFAP were seen near the surface in TG mice. D. Increased GluR2 expressions in GFAP expressing regions. E. Merged image of C and D. F. Calbindin immunostaining in TG mice. Note normal elaboration of Purkinje cell dendrites. G. GluR2 immunostaining. H. Merged image of F and G. Scale bars indicate 50 micrometer.

power of the GFA2 promoter is approximately one third of that of CMV promoter, depending on the host cells used (29). Our results matched with their reports. The expressions of GluR2 in TG mice were prominent in BG cells (Figure 3), which lack the expression of GluR2. The expression in type-1 astrocytes, which intrinsically express GluR2 at a low level, was also increased, 1.9 – 2.1 folds at the mRNA level and 4.2 folds at the protein level (Figure 2). The expression of GluR2 in type-1 astrocytes is not strong (31), compared with that in neurons, indicating the

power of GFAP promoter is not strong compared with the power of promoter of AMPA receptor subunits. We did not found changes of GluR2 extracted from the brain both in mRNA and in proteins of the forebrain and cerebellum (Figure 4), suggesting that changes of GluR2 were not occurred in neuronal cells, which abundantly express GluR2. BG cells abundantly express GluR1 and GluR4, and functional AMPA receptor currents could be recorded in these cells (7,10). This result might challenge our previous report that GluR2 expression using adenovirus
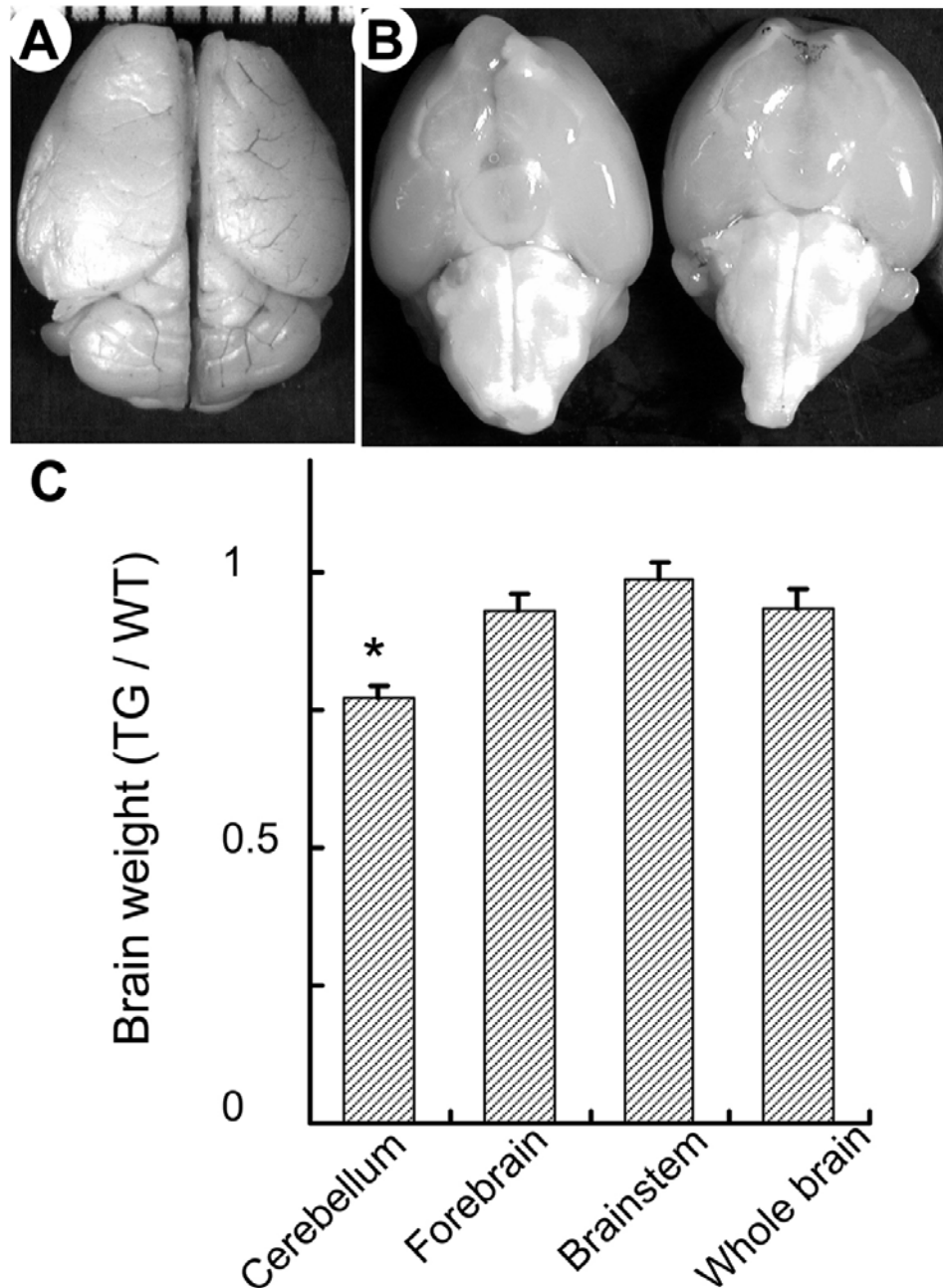
Figure 6. Reduced brain size in TG mice. A. Macro image of brains of WT (left hemisphere) and TG (right hemisphere). The scale in the top is in 1 mm intervals. B. Macro image of WT (left) and TG (right) viewed from downside. The forebrain are smaller in TG mice, in contrast, the brainstem appears to be similar. C. Relative brain weight of TG mice compared with WT mice. * indicate significant ($p < 0.05$) differences in Student's t-test.

vector changes the electrophysiological properties in the BG cells (10). We had used a CAG promoter that derived from CMV promoter (32) for the expression of GluR2 in adenoviral expression system. Stronger promoter than that of AMPA receptors would be required to change electrophysiological properties of BG cells. Recently, GFA2 promoter was used to activate strong promoter restricted in GFAP expressing cells (33), and it would be performed in further studies.

5.2. Changes of expression of GFAP in the molecular layer of the cerebellum

Focal wedge-shaped expressions of GFAP were seen near the surface in TG mice in addition with normal thin vertical expressions (Figure 5C). Similar expression patterns were found in all three lines obtained in the present study, indicating that this phenotype is not an artifact of the transgene integration site. Although overall GluR2 expression is upregulated in BG cells, focal expressions of
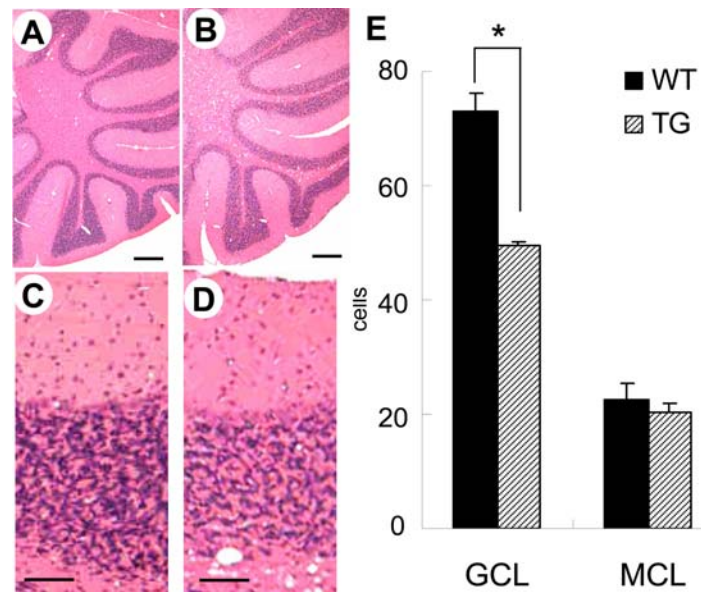
Figure 7. Reduced cell numbers in cerebellar cortex. A-D. H-E staining of the cerebellum cortex of WT mice (lower magnification; A, higher magnification C) and TG mice (B, D, lower and higher magnification, respectively). Sagittal slices were made from paraffin embedded blocks and sectioned at 3 micrometer thickness. Bars 100 micrometer in A and B and 50 micrometer in C and D. Note reduced number of cells in granule cell layer. E. The number of cells in 50 micrometer square was counted in six different slices. GCL: granule cell layer. MCL; molecular cell layer. * indicate significant ($p < 0.05$) differences in Student's t-test.
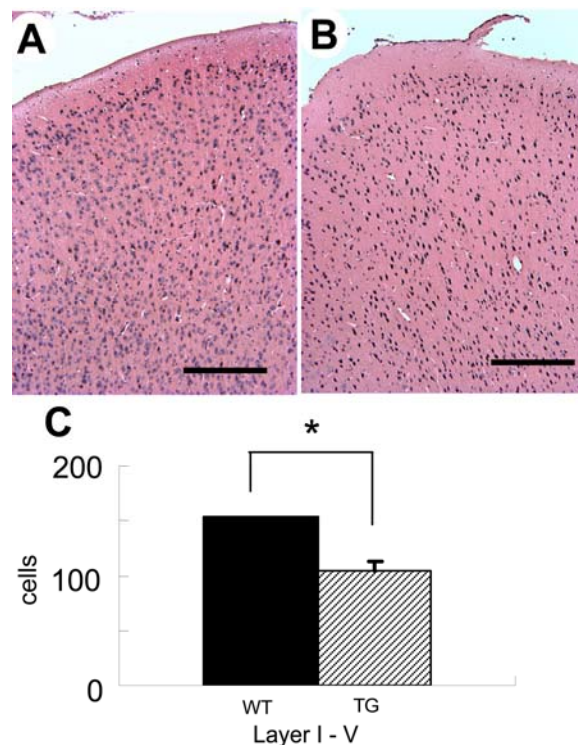

Figure 8. Reduced cell numbers in somatosensory cortex. A-B. H-E staining of the somatosensory cortex of WT mice (A) and TG mice (B). The paraffin embedded blocks were sectioned at 3 micrometer thickness. Bars 100 micrometer. C. The numbers of cells in 150 micrometer lengths from the surface, including cells in layer I to V, 50 micrometer widths were counted in six different slices. * indicate significant ($p < 0.05$) differences in Student's t-test.

GluR2 in wedge shaped area suggest that BG cells have different regulatory mechanisms for controlling GFAP expression each other.

In the GFAP foci, the expression of GluR2 was markedly increased (Figure 5E), showing that transcription factors acting on the intrinsic GFAP promoter are similarly acting on the GFA-GluR2 construct. In spite of the presence of GFAP foci, dendrites of Purkinje cells seem not to be affected (Figure 5H). Abnormal expression of GluR2 observed in the upper molecular layers was always associated with retracted or tangled irregular GFAP-positive BG fibers. Taking the findings of culture experiments shown in Figure 3 into consideration, GluR2 subunits would hinder the branching of normal glial processes.

5.3. Decreases of neurons in TG mice brain

We found reduced number of neurons in cerebellum and in cerebral cortex (Figs 7-8), which resulted in reduced brain weight (Figure 6). These results would indicate that GluR2 expression in GFAP- positive cells in a developing brain influences the number of neurons in the cerebellum and the cerebral cortex. The number of neurons was reduced in the cerebellum and the forebrain but the brainstem was not reduced. McCall *et al* reported that astrocyte precursors initially express vimentin, then switching to GFAP as they mature (34). In accordance with glial development, the region developed in the later stage was more strongly affected than that of early developmental stage in our TG mice.

In neuro-glial interaction, glial processes play an important role. They form coverage of synapses and modulate electrical conduction. They form vascular foots on vessels to supply energy fuel and nutrients for surrounding neurons. Since the overexpression of GluR2 reduces these contacts of BG processes (10), introduction of GluR2 gene in GFAP expressing cells might reduce survivals of neuronal cells. Bergmann glia and radial glia are known to their contribution of the guiding substrate of neuronal cells. Their special characteristics of long radial array extension of cellular processes were disrupted by GluR2. It may result in the reduced number of neurons in the cerebellum and the cerebrum.

Another possibility is that GluR2 expressed in neuronal precursor cells might effect the number of neurons in adult. Although GFAP is an intermediate filament protein found in glial cells, GFAP is also expressed in progenitor cells that give rise to neurons in the cerebral cortex. (26,35). At the present time, these two possibilities are similar likely. TG mice that express GluR2 at any desirable time would be required in the further study.

6. ACKNOWLEDGMENT

7. REFERENCES

1. S. Ozawa, H. Kamiya and K. Tsuzuki: Glutamate receptors in the mammalian central nervous system. *Prog Neurobiol* 54, 581-618 (1998)

2. P. Bochet, E. Audinat, B. Lambolez, F. Crepel, J. Rossier, M. Iino, K. Tsuzuki and S. Ozawa: Subunit composition at the single-cell level explains functional properties of a glutamate-gated channel. *Neuron* 12, 383-388 (1994)

3. J. R. Geiger, T. Melcher, D. S. Koh, B. Sakmann, P. H. Seeburg, P. Jonas and H. Monyer: Relative abundance of subunit mRNAs determines gating and Ca^{2+} permeability of AMPA receptors in principal neurons and interneurons in rat CNS. *Neuron* 15, 193-204 (1995)

4. P. Jonas, C. Racca, B. Sakmann, P. H. Seeburg and H. Monyer: Differences in Ca^{2+} permeability of AMPA-type glutamate receptor channels in neocortical neurons caused by differential GluR-B subunit expression. *Neuron* 12, 1281-1289 (1994)

5. S. Shi, Y. Hayashi, J. A. Esteban and R. Malinow: Subunit-specific rules governing AMPA receptor trafficking to synapses in hippocampal pyramidal neurons. *Cell* 105, 331-343 (2001)

6. Z. Jia, N. Agopyan, P. Miu, Z. Xiong, J. Henderson, R. Gerlai, F. A. Taverna, A. Velumian, J. MacDonald, P. Carlen, W. Abramow-Newerly and J. Roder: Enhanced LTP in mice deficient in the AMPA receptor GluR2. *Neuron* 17, 945-956 (1996)

7. N. Burnashev, A. Khodorova, P. Jonas, P. J. Helm, W. Wisden, H. Monyer, P. H. Seeburg and B. Sakmann: Calcium-permeable AMPA-kainate receptors in fusiform cerebellar glial cells. *Science* 256, 1566-1570 (1992)

8. S. Ishiuchi, K. Tsuzuki, N. Yamada, H. Okado, A. Miwa, H. Kuromi, H. Yokoo, Y. Nakazato, T. Sasaki and S. Ozawa: Extension of glial processes by activation of Ca^{2+}-permeable AMPA receptor channels. *Neuroreport* 12, 745-748 (2001)

9. K. Matsui, C. E. Jahr and M. E. Rubio: High-concentration rapid transients of glutamate mediate neural-glial communication via ectopic release. *J Neurosci* 25, 7538-7547 (2005)

10. M. Iino, K. Goto, W. Kakegawa, H. Okado, M. Sudo, S. Ishiuchi, A. Miwa, Y. Takayasu, I. Saito, K. Tsuzuki and S. Ozawa: Glia-synapse interaction through Ca^{2+}-permeable AMPA receptors in Bergmann glia. *Science* 292, 926-929 (2001)

11. M. Brenner, W. C. Kisseberth, Y. Su, F. Besnard and A. Messing: GFAP promoter directs astrocyte-specific expression in transgenic mice. *J Neurosci* 14, 1030-1037 (1994)

12. M. Higuchi, F. N. Single, M. Kohler, B. Sommer, R. Sprengel and P. H. Seeburg: RNA editing of AMPA

receptor subunit GluR-B: a base-paired intron-exon structure determines position and efficiency. Cell 75, 1361-1370 (1993)

13. B. Sommer, K. Keinanen, T. A. Verdoorn, W. Wisden, N. Burnashev, A. Herb, M. Kohler, T. Takagi, B. Sakmann and P. H. Seeburg: Flip and flop: a cell-specific functional switch in glutamate-operated channels of the CNS. *Science* 249, 1580-1585 (1990)

14. H. Lomeli, J. Mosbacher, T. Melcher, T. Hoger, J. R. Geiger, T. Kuner, H. Monyer, M. Higuchi, A. Bach and P. H. Seeburg: Control of kinetic properties of AMPA receptor channels by nuclear RNA editing. *Science* 266, 1709-1713 (1994)

15. J. Boulter, M. Hollmann, A. O'Shea-Greenfield, M. Hartley, E. Deneris, C. Maron and S. Heinemann: Molecular cloning and functional expression of glutamate receptor subunit genes. *Science* 249, 1033-1037 (1990)

16. M. Noble and M. Mayer-Proschel, Culture of astrocytes, oligodendrocytes, and O-2A progenitor cells. (In G. Banker and Goslin K, Eds) Culturing Nerve Cells, 2nd edition pp 499 -543. The MIT Press, Cambridge, MA (1998)

17. K. Tsuzuki, B. Lambolez, J. Rossier and S. Ozawa: Absolute quantification of AMPA receptor subunit mRNAs in single hippocampal neurons. *J Neurochem* 77, 1650-1659 (2001)

18. Q. Chou, M. Russell, D. E. Birch, J. Raymond and W. Bloch: Prevention of pre-PCR mis-priming and primer dimerization improves low-copy-number amplifications. *Nucleic Acids Res* 20, 1717-1723 (1992)

19. Z.Govindarajulu, Statistical Techniques in Bioassay. Karger, Basel, Switzerland (2001)

20. C. A. Heid, J. Stevens, K. J. Livak and P. M. Williams: Real time quantitative PCR. *Genome Res* 6, 986-994 (1996)

21. M. C. Angulo, B. Lambolez, E. Audinat, S. Hestrin and J. Rossier: Subunit composition, kinetic, and permeation properties of AMPA receptors in single neocortical nonpyramidal cells. *J Neurosci* 17, 6685-6696 (1997)

22. B. Lambolez, E. Audinat, P. Bochet, F. Crepel and J. Rossier: AMPA receptor subunits expressed by single Purkinje cells. *Neuron* 9, 247-258 (1992)

23. S. Ishiuchi and M. Tamura: Central neurocytoma: an immunohistochemical, ultrastructural and cell culture study. *Acta Neuropathol* (Berl) 94, 425-435 (1997)

24. C. Nolte, M. Matyash, T. Pivneva, C. G. Schipke, C. Ohlemeyer, U. K. Hanisch, F. Kirchhoff and H. Kettenmann: GFAP promoter-controlled EGFP-expressing transgenic mice: a tool to visualize astrocytes and astrogliosis in living brain tissue. *Glia* 33, 72-86 (2001)

25. L. Zhuo, B. Sun, C. L. Zhang, A. Fine, S. Y. Chiu and A. Messing: Live astrocytes visualized by green fluorescent protein in transgenic mice. *Dev Biol* 187, 36-42 (1997)

26. Y. M. Ganat, J. Silbereis, C. Cave, H. Ngu, G. M. Anderson, Y. Ohkubo, L. R. Ment and F. M. Vaccarino: Early postnatal astroglial cells produce multilineage precursors and neural stem cells *in vivo. J Neurosci* 26, 8609-8621 (2006)

27. C. L. Delaney, M. Brenner and A. Messing: Conditional ablation of cerebellar astrocytes in postnatal transgenic mice. *J Neurosci* 16, 6908-6918 (1996)

28. S. Ishiuchi, K. Tsuzuki, Y. Yoshida, N. Yamada, N. Hagimura, H. Okado, A. Miwa, H. Kurihara, Y. Nakazato, M. Tamura, T. Sasaki and S. Ozawa: Blockage of Ca^{2+}-permeable AMPA receptors suppresses migration and induces apoptosis in human glioblastoma cells. *Nat Med* 8, 971-978 (2002)

29. B. de Leeuw, M. Su, M. ter Horst, S. Iwata, M. Rodijk, R. C. Hoeben, A. Messing, P. S. Smitt and M. Brenner: Increased glia-specific transgene expression with glial fibrillary acidic protein promoters containing multiple enhancer elements. *J Neurosci* Res 83, 744-753 (2006)

30. F. Doetsch, I. Caille, D. A. Lim, J. M. Garcia-Verdugo and A. Alvarez-Buylla: Subventricular zone astrocytes are neural stem cells in the adult mammalian brain. *Cell* 97, 703-716 (1999)

31. D. Fan, S. Y. Grooms, R. C. Araneda, A. B. Johnson, K. Dobrenis, J. A. Kessler and R. S. Zukin: AMPA receptor protein expression and function in astrocytes cultured from hippocampus. *J Neurosci* Res 57, 557-571 (1999)

32. H. Niwa, K. Yamamura and J. Miyazaki: Efficient selection for high-expression transfectants with a novel eukaryotic vector. *Gene* 108, 193-199 (1991)

33. P. Ye, G. J. Popken, A. Kemper, K. McCarthy, B. Popko and A. J. D'Ercole: Astrocyte-specific overexpression of insulin-like growth factor-I promotes brain overgrowth and glial fibrillary acidic protein expression. *J Neurosci* Res 78, 472-484 (2004)

34. M. A. McCall, R. G. Gregg, R. R. Behringer, M. Brenner, C. L. Delaney, E. J. Galbreath, C. L. Zhang, R. A. Pearce, S. Y. Chiu and A. Messing: Targeted deletion in astrocyte intermediate filament (Gfap) alters neuronal physiology. *Proc Natl Acad Sci U S A* 93, 6361-6366 (1996)

35. K. B. Casper and K. D. McCarthy: GFAP-positive progenitor cells produce neurons and oligodendrocytes throughout the CNS. *Mol Cell Neurosci* 31, 676-684 (2006)

Send correspondence to: Shogo Ishiuchi, MD & PhD, Department of Neurosurgery, Gunma University Graduate School of Medicine, 3-39-22 Showa-machi, Maebashi, Gunma, 371-8511, Japan, Tel 81-72-20-8515, Fax: 81-272-20-8525, E-mail: ishogo@showa.gunma-u.ac.jp